

Friction–Wear Characteristics of High Velocity Oxygen Fuel Sprayed NiCrBSi Alloy Coating at Elevated Temperatures

Zhao Wen¹ · Benguo Zhao¹ · Dejun Kong¹ 

Received: 25 March 2018 / Accepted: 9 July 2018 / Published online: 23 July 2018
© The Indian Institute of Metals - IIM 2018

Abstract A NiCrBSi alloy coating was sprayed on H13 hot work mould using a high velocity oxygen fuel. The surface and cross-section morphologies of obtained NiCrBSi coating were observed using a field emission scanning electron microscope (SEM), its phases were analyzed using an X-ray diffractometer (XRD). The friction-wear behaviors of NiCrBSi coating were investigated using a high temperature wear tester, the morphologies and chemical elements of worn tracks were analyzed using a SEM and its configured energy dispersive spectrometer (EDS), respectively. The results show that the average COF of NiCrBSi coating at 500, 600, and 700 °C is 0.4046, 0.4039, and 0.3975, respectively. The wear mechanism of NiCrBSi coating at 500 and 600 °C is abrasive wear, adhesive wear and oxidation wear, while that at 700 °C is abrasive wear and oxidation wear, the wear resistance of NiCrBSi coating is dependent on the compounds of Ni, Si and Cr.

Keywords High velocity oxygen fuel (HVOF) · NiCrBSi coating · COF (coefficient of friction) · Wear performance

1 Introduction

H13 hot work mould steel has good hardenability, anti-tempering stability, wear resistance and heat resistance, which is widely used in the manufacture of hot extrusion,

hot forging, die casting and isothermal forging mould [1, 2]. Its wear form is primarily hot wear, accompanied with adhesive wear and abrasive wear under the working conditions [3]. Surface treatment technology is used to solve the hot wear problems, which includes deformation strengthening, heat treatment, chemical heat treatment, surface metallurgical strengthening, etc. Among those, the surface coating technique is one kind of surface metallurgical strengthening, which effectively improves its friction and wear performance at high temperatures [4].

Thermal spraying is one of the main methods for fabricating the above coatings, which includes plasma spraying, flame spraying, arc spraying, coating technique of powder metallurgy (induction melting) and laser cladding [5, 6]. Among them, high velocity oxygen fuel (HVOF) is heated evenly, melted fully and sprayed quickly [7–9], and is suitable for spray coating with high bonding strength [10]. As a Ni-based coating, NiCrBSi coating has excellent advantages such as uniform microstructure, high wear resistance and oxidation resistance at high temperatures [11–13]. Karaoglanli et al. [14] analyzed the friction and wear properties of HVOF sprayed NiCrBSi/WC coatings under dry friction conditions; Houdková et al. [15] evaluated the microstructure, hardness, elastic modulus and wear resistance of NiCrBSi coating before and after heat treatment; Guo et al. [16] investigated the friction and wear behavior of laser cladded NiCrBSi coating and NiCrBSi/WC–Ni composite coatings at 500 °C; Shabana et al. [17] evaluated the wear resistance of HVOF sprayed coatings at 350 °C. The above researches on the NiCrBSi coating was mainly focused on the preparation method, and its wear properties was also limited to room temperature or 350 and 500 °C. There were few studies on the effect of elevated temperatures on its friction and wear performance.

✉ Dejun Kong
kong-dejun@163.com

¹ School of Mechanical Engineering, Changzhou University, Changzhou 213164, China

In order to solve the hot wear problem of H13 hot work mould steel, a HVOF sprayed NiCrBSi coating was fabricated on its surface. The friction and wear performance at 500, 600 and 700 °C were investigated using a plane scan analysis, wishing that the application of NiCrBSi coating could reduce friction and decrease wear of H13 hot work mould steel.

2 Experimental

The substrate was H13 hot mould steel with the chemical composition (mass fraction, %) of: Cr 4.75–5.00, Si 0.80–1.20, Mo 1.10–1.72, V 0.80–1.20, C 0.32–0.45, the rest was Fe. The samples were cleaned with acetone to remove oil, and roughened with brown corundum. Powder material was Ni-based self-melted alloy of NiCrBSi with the chemical composition (mass fraction, %) of: Cr 15.80, B 3.07, Si 4.53, Fe 5 and C 0.79, the rest was Ni, and its particle size distribution was measured using a Mastersizer 3000 type laser particle size analyzer. Before HVOF spraying, the samples were pretreated at 120 °C for 1 h. The HVOF test was conducted on a ZB-2700 type high speed flame spraying device, aviation kerosene was used as fuel, O₂ gas as combustion supporting gas, and N₂ gas as feeding powder. Spraying parameters were: powder feeding amount of 110 g/min, spray gun distance of 250 mm, fuel pressure of 1.25 MPa, O₂ pressure of 1.58 MPa, water temperature of 40 °C, spraying pressure of 0.95 MPa. After the HVOF spraying, the hardness of the obtained coating and substrate was measured using a HVS-1000 type vickers hardness tester. The technological parameters were: experimental force of 2 N, holding time of 10 s. The high temperature friction–wear test was performed on a HT-1000 type high temperature friction and wear tester with technological parameters as: friction pair of Si₃N₄ ceramic ball with the diameter of 5 mm, wear load of 10 N, time of 60 min. Respective temperatures were: 500, 600, and 700 °C. After the wear test, the profiles worn tracks were measured using a VHX-700FC type super-depth three-dimensional microscopic system. Their morphologies and chemical elements were analyzed with a JSM-6360LA type SEM and configured EDS, respectively, and the phases were measured on a D/max 2500PC type XRD.

3 Analysis and Discussion

3.1 Morphologies and XRD Analysis of Powders

The sprayed NiCrBSi powder presented the spherical or nearly spherical shapes, as shown in Fig. 1a. The surface roughness was low, which was advantageous to transport

the powder in the HVOF spraying test. The NiCrBSi coating was easily formed through HVOF flame flow. Figure 1b shows that distribution of NiCrBSi particle sizes. The NiCrBSi powders were distributed in the range of 5–80 μm, the particle diameter of 30–55 μm accounted for 84.5% of total volume fractions, which was beneficial in increasing its liquidity. Figure 1c shows the XRD spectra of NiCrBSi powder. The sprayed powder was composed of B, Ni₄B₃, Ni₂Si, Cr₂Si, Ni, Cr₂Ni₅Si₂, Si, Cr₂Ni₂Si₂, and Cr₂B. The surface smoothness of sprayed powder was well; only a small part of depressions existed, which was primarily due to the existence of B and Si phases. The B and Si formed the eutectic with the Ni and Fe, decreasing the melting point of NiCrBSi alloy powder. Its wettability to the substrate was improved [18].

3.2 Surface and Cross-Section Morphologies and XRD Analysis

The morphology of obtained NiCrBSi coating surface is shown in Fig. 2a. The surface roughness was good, the sprayed powder was completely melted, its porosity was low. The morphology of NiCrBSi coating cross-section is shown in Fig. 2b. The microstructure of NiCrBSi coating cross-section was uniform and compact, its thickness was ~ 400 μm. Figure 2c shows the XRD spectra of NiCrBSi coating. It was primarily composed of Ni, Ni₂B, Ni₂Si, and NiSi₂ phases. The spectral line was wide, but the diffraction peak of each phase was not obvious. The following reactions occurred during the HVOF spraying test.



The stable NiSi₂ and Ni₂B were formed in Eqs. (1) and (2), the micro-crystalline/amorphous structure and micro strain were the main broadening cause of XRD peaks. In addition, the grain dislocation and twin defects also caused the XRD peaks broaden. Among those, the micro-crystal and amorphous was produced because the NiCrBSi powder was heated to the melted or semi-melted in the HVOF flow, and was pushed to the substrate surface by the flame flow, the solidification was so rapid that the crystal did not spread and solidified with the disordered state.

3.3 Microhardness

Figure 3a shows the microhardness of NiCrBSi coating and substrate, which was the average of values taken from five points. The average microhardness of substrate was 614 HV, while that of NiCrBSi coating was 858 HV, which got increased by 39.7% than the substrate. Figure 3b shows the microhardness distribution of NiCrBSi coating in the depth

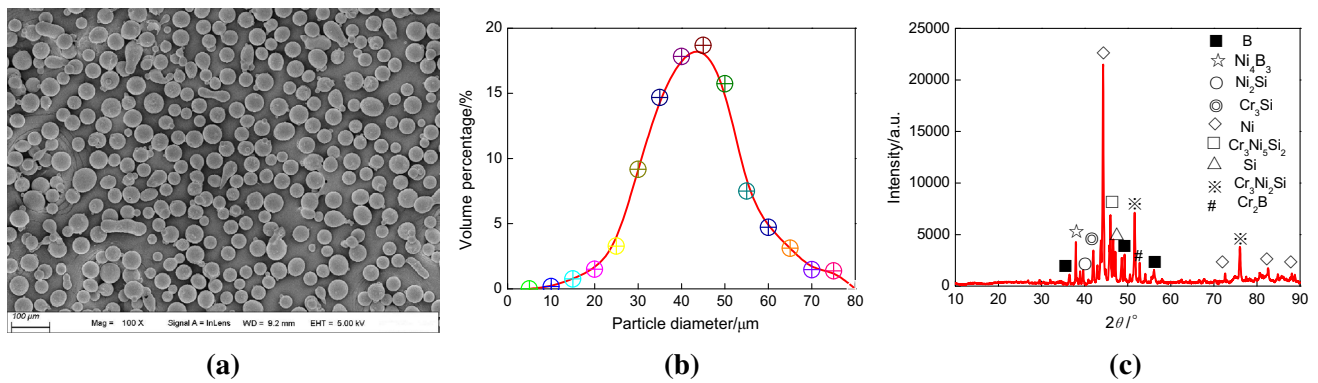


Fig. 1 Morphology, distribution of particle sizes and XRD analysis of NiCrBSi powder. **a** Morphologies of NiCrBSi powder. **b** Distribution of particle sizes. **c** XRD analysis

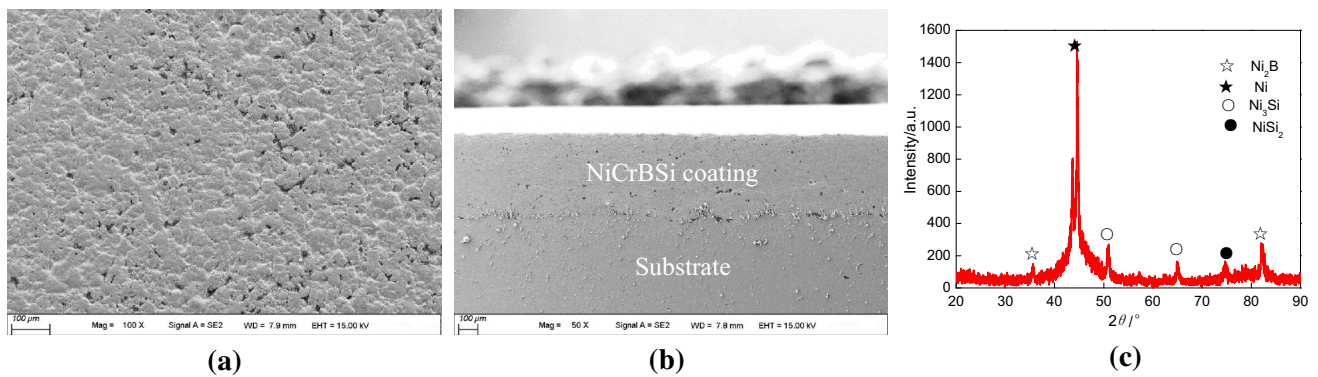
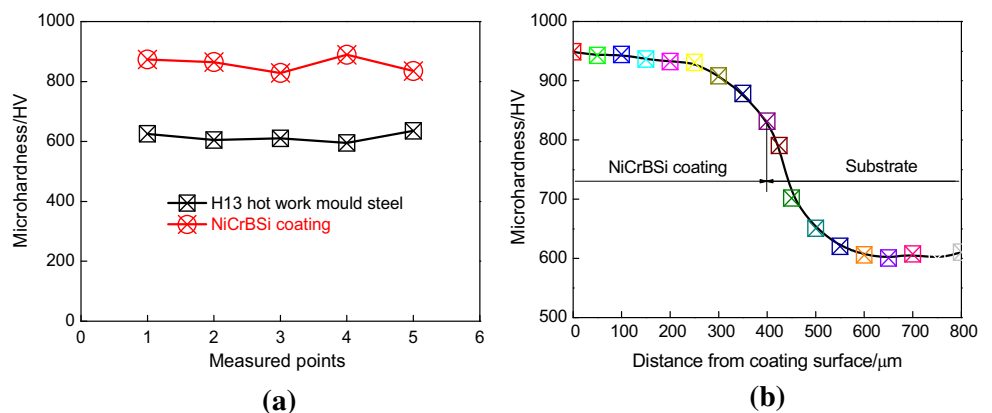


Fig. 2 Surface and cross-section morphologies and XRD analysis of NiCrBSi coating. **a** Surface morphology. **b** Cross-section morphology. **c** XRD analysis

Fig. 3 Microhardness of NiCrBSi coating surface and depth. **a** Hardness on coating surface. **b** Hardness in coating depth direction

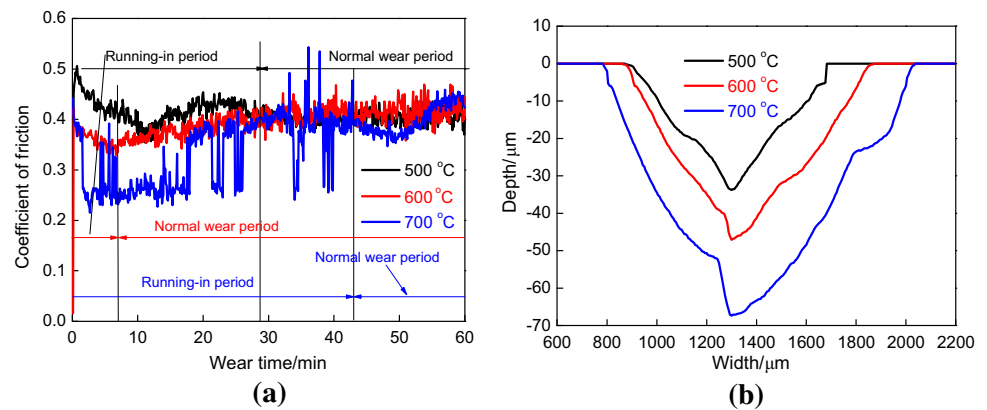


direction. The microhardness on the NiCrBSi cross-section basically remained ~ 820 HV, which decreased gradually at the substrate/coating interface and eventually decreased to the microhardness of the substrate. The difference in microhardness between the NiCrBSi and the substrate was because the compounds of Ni Cr, B and Si were formed to enhance its microhardness [19] and improve its wear resistance.

3.4 COFs and Profiles of Worn Tracks

Figure 4a shows the curves of COFs versus wear time at different high temperatures. The wear process was divided into two periods, i.e., running-in period and normal wear period. When the wear test was over, the COFs were not fluctuated, which indicated that the NiCrBSi coating did not fail. It was shown that: (1) during the running-in period, the COFs were large due to its surface roughness.

Fig. 4 COFs versus wear time and profiles of worn tracks at different high temperatures.
a COFs versus wear time.
b Profiles of worn tracks



When the Ni on the worn track was oxidized into NiO and NiO₂, playing a role of lubrication, the COFs began to decrease and was tended to become stable; (2) at 500 °C, the running-in time of 29 min was longer, the average COF was 0.4179, while that in the normal wear period was 0.4046; (3) at 600 °C, the running-in time of 8 min was shorter, the average COF was 0.3574, while that in the normal wear period was 0.4039, which was the result of uneven distribution of hard phases; (4) at 700 °C, the running-in time of 42 min was long, the COFs varied greatly, its average value was 0.3304, while that in the normal wear period was 0.3975. From the above analysis, it could be seen that the COFs in the normal wear period decreased slightly with the increase of temperature, but there was little difference in COFs at each temperature. Because the running-in time at 600 °C was obviously less than the other two temperatures and the COF curve was the most stable, the friction performance of NiCrBSi coating at 600 °C was the best.

Figure 4b shows the profiles of worn tracks at the different temperatures. The wear volume of NiCrBSi coating at 500, 600, and 700 °C was 0.3687, 0.7506, and 1.4087 mm³, respectively, showing that the NiCrBSi coating had low wear resistance at 700 °C. The depth of worn tracks did not exceed the thickness of NiCrBSi coating at all the three temperatures, indicating that the NiCrBSi coating effectively protected the substrate under a load of 10 N, and had good wear resistance.

3.5 Worn Morphologies

Figure 5 shows the wear morphologies of NiCrBSi coating at the different temperatures. A part of NiCrBSi coating was spalled off at the high temperatures, the main feature under the oxidation and friction contact was the furrow and flaking. The furrow width at 500 °C was large, as shown in Fig. 5a. The furrow width at 600 °C was smaller than that at 500 °C, as shown in Fig. 5b. There were few worn furrows distributed on both sides of the worn track at

700 °C. The central zone was smooth with less flaking, as shown in Fig. 5c. The above analysis shows that: (1) at 500 and 600 °C, the wear mechanism was primarily adhesive wear and abrasive wear accompanied with oxidation wear, while that was primarily abrasive wear and oxidation wear at 700 °C; (2) during the wear test, the friction heat was produced to oxidize the Cr and Si at 500 and 600 °C, but the produced oxide was brittle could easily be crushed under the wear load. The oxide film formed at 700 °C was dense, and a small amount of peeling and flaky pits were formed on the worn track, its average COF was the minimum; (3) the oxidation and spalling on the worn track were not regular, and the furrows and spalling were produced under the action of continuous wear loads.

At 500 and 600 °C, the minority of worn track was oxidized, the size of oxidized particles was less than 1 μm, as shown in Fig. 6a, b. A large number of oxidized flakes appeared on the worn track at 700 °C, forming a dense oxide film. During the dry wear, the friction pair surface generated the oxide film, which was made by grinding and refining [20–24]. The oxide film played a role of bearing, and avoided the direct contact between the NiCrBSi coating and the substrate. The wear mechanism was changed from severe adhesive wear to slight oxidation wear. At the same time, the oxide film bearing capacity increased with the increased oxidation. At 700 °C, the worn track surface was smooth, no furrow was observed which was consistent with the above analysis results. According to the Wilson theory [25], the oxide film was not stable in the high temperature wear test, the fatigue spalling occurred under the repeated action of wear stress. The wear was a cyclic process of oxide film generating-spalling off and regenerating. The wear debris was removed in the wear test, therefore, the wear mechanism was wear loss.

Figure 7 shows the EDS analysis of oxidized particles at different temperatures. The mass fractions and atomic fractions of chemical elements are shown in Table 1. The mass fraction of O on the worn tracks at three temperatures were less than 10%. Among them, it was 8.56% at 700 °C.

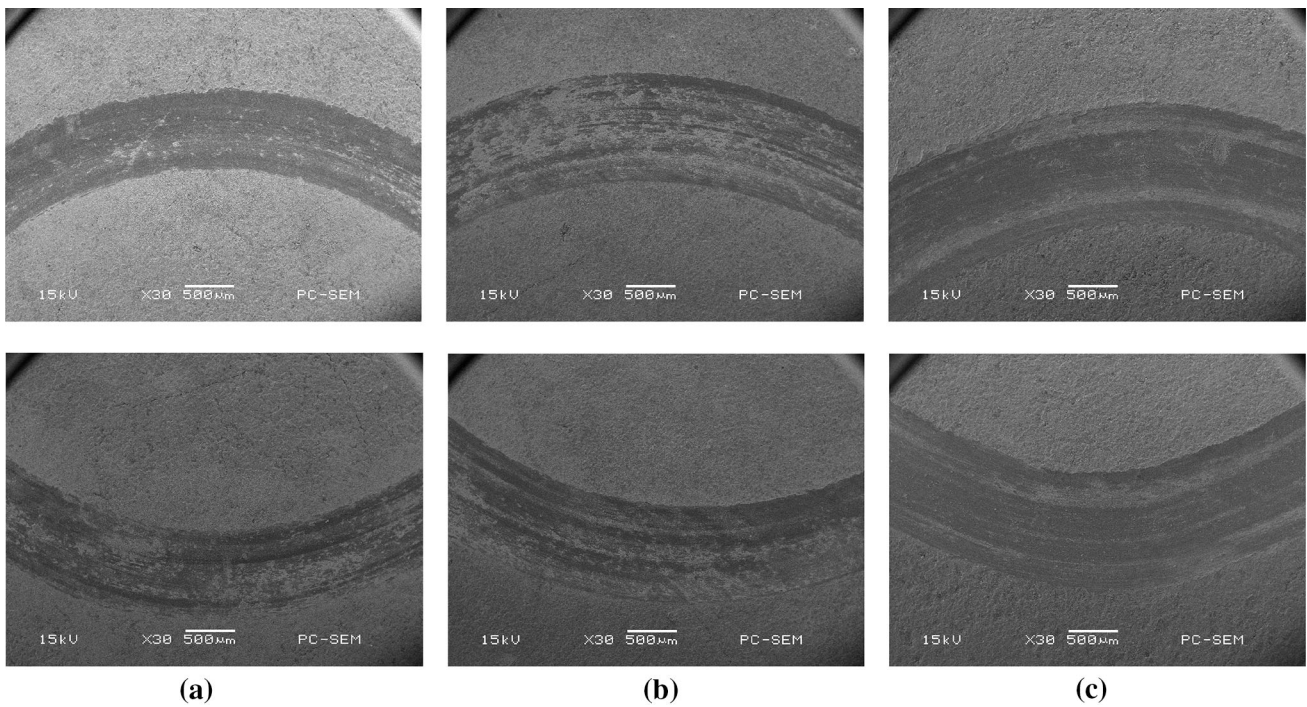


Fig. 5 Overall SEM images of worn tracks at different high temperatures. **a** At 500 °C. **b** At 600 °C. **c** At 700 °C

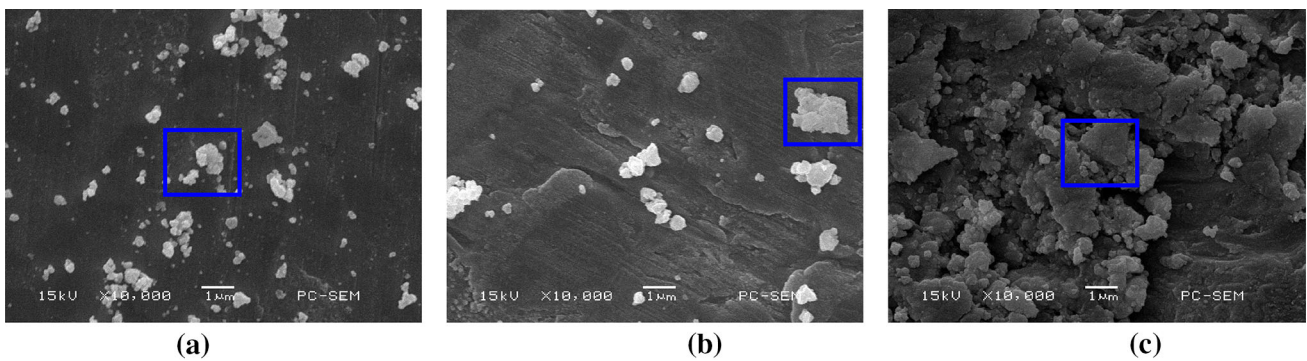


Fig. 6 Oxidation morphologies of NiCrBSi coating at different high temperatures. **a** At 500 °C. **b** At 600 °C. **c** At 700 °C

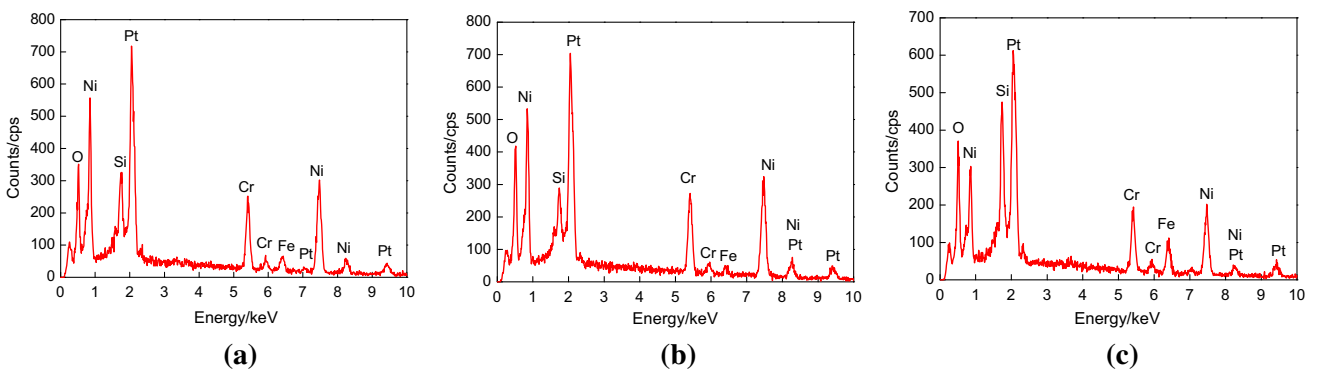


Fig. 7 EDS analysis of oxide particles on NiCrBSi coating at different high temperatures. **a** At 500 °C. **b** At 600 °C. **c** At 700 °C

Table 1 EDS analysis results of oxide particles on worn tracks at different high temperatures

Element	500 °C		600 °C		700 °C	
	Mass/%	At/%	Mass/%	At/%	Mass/%	At/%
C	–	–	–	–	7.46	15.13
O	6.21	18.38	8.10	23.21	8.56	20.41
Si	4.37	7.36	3.39	5.53	8.99	12.21
Cr	18.42	16.77	19.96	17.60	16.21	11.89
Fe	5.67	7.81	2.98	2.45	12.53	8.56
Ni	65.32	52.67	65.57	51.21	48.95	31.81

The NiCrBSi coating had better oxidation resistance at the high temperature.

3.6 XRD Analysis on Worn Tracks

Figure 8 shows the XRD spectra of worn tracks at different high temperatures. The phase analysis results indicated that: (1) there was Ni phase on the worn tracks at three high temperatures, and the Ni oxide and other hard phases also appeared; (2) The Ni was oxidized into NiO at 500 °C (Fig. 8a), while Ni was oxidized into the two oxides of NiO and NiO₂ at 600 and 700 °C (Fig. 8b, c), which played a certain role in reducing COFs; (3) there was a Cr₃B₄ on the worn track at 500 °C, while there was the NiSi₂ on the worn track at 600 °C, and there was the Si on the worn track at 700 °C. Among those, the Cr₃B₄ and Si improved the microhardness of NiCrBSi the coating, and the NiSi₂ had good thermal stability at high temperatures.

3.7 Plane Scan Analysis of Worn Tracks

Figure 9a shows the plane scanned position of worn track at 500 °C. The surface of worn track was intact without cracks, but there were obvious furrows with adhesion phenomenon. The result of plane scan analysis is shown in Fig. 9b. The mass fractions of chemical elements were

(mass%): Ni 69.63, Cr 21.80, Si 2.55, O 2.43 and Fe 3.59; and the corresponding atomic fractions were (at%): Ni 62.03, Cr 21.93, Si 4.75, O 7.93 and Fe 3.36. Among them, B was not present because it is a light element and because of its low content, while the Fe was the impurity which came from the diffusion of substrate during the HVOF spraying test, which could be ignored in the wear test. The Ni and Si were uniformly distributed on the worn track, with no atom-poor zones, as shown in Fig. 9c, e. The Cr formed the atom-rich zone on the worn track, indicating that the Cr and its compounds were the main factor of wear resistance, as shown in Fig. 9d. O was present on the worn track; this was because the friction heat caused the elements of substrate to react with the O in the air to produce the oxide, which was uniformly distributed on the worn track, as shown in Fig. 9f.

Figure 10a shows the plane scanned position of worn track at 600 °C. The width of worn track increased than that at 500 °C, however, the grooves and spalling decreased at a certain extent. The result of plane scan analysis is shown in Fig. 10b. The mass fractions of chemical elements (mass%) were: Ni 67.02, Cr 23.82, Si 3.13, O 2.54 and Fe 3.49; and the corresponding atomic fractions (at%) were: Ni 59.08, Cr 23.71, Si 5.76, O 8.22 and Fe 3.23. Among them, B also was not present. This was because, B belongs to light element group and its

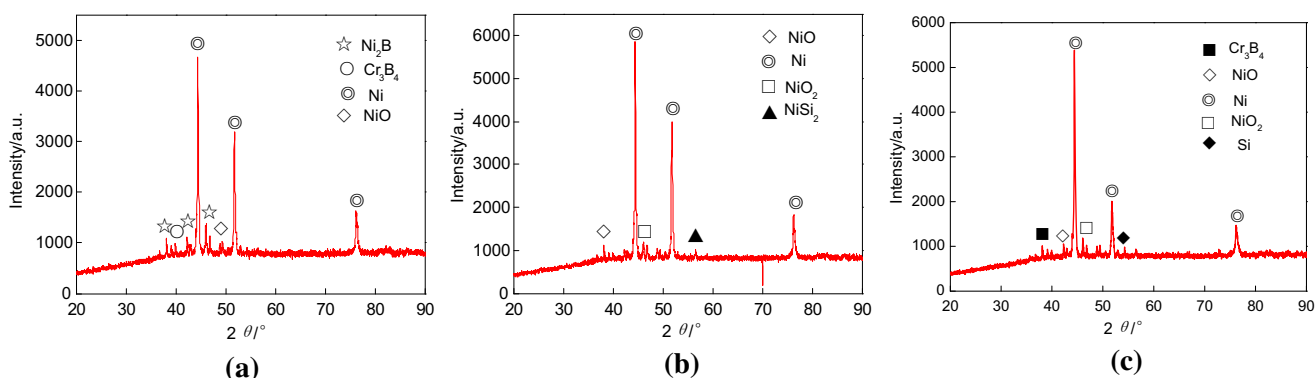


Fig. 8 XRD analysis of worn tracks at different high temperatures. **a** At 500 °C. **b** At 600 °C. **c** At 700 °C

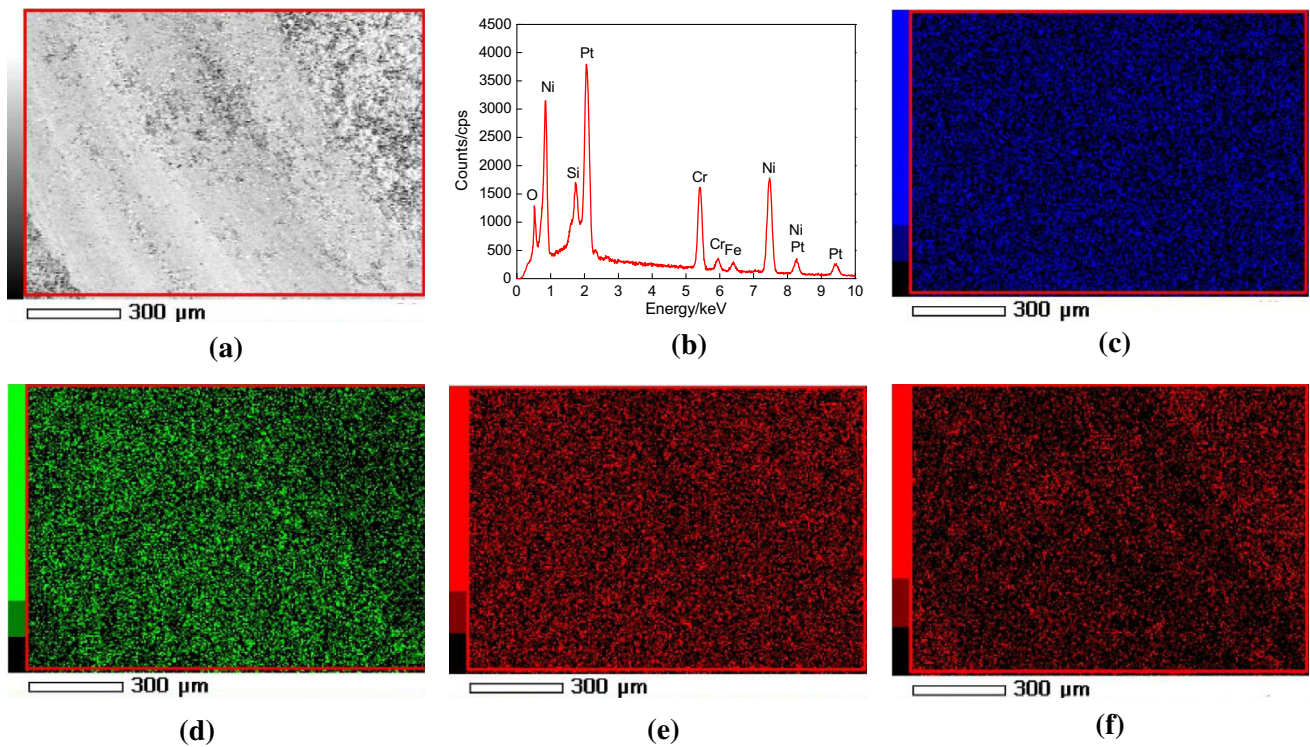


Fig. 9 Plane scan analysis of worn track at 500 °C. **a** Plane scanned position. **b** Result of plane scan analysis. **c** Ni content. **d** Cr content. **e** Si content. **f** O content

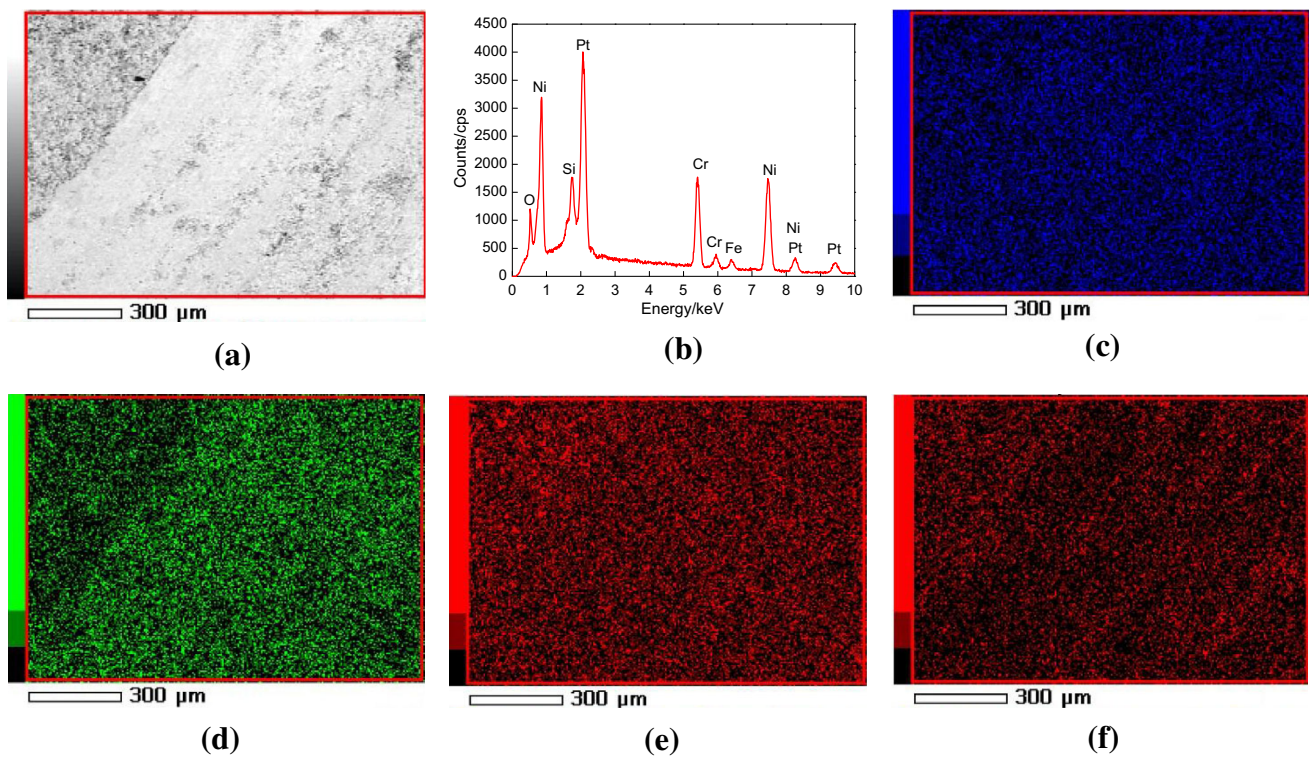


Fig. 10 Plane scan analysis of worn track at 600 °C. **a** Plane scanned position. **b** Result of plane scan analysis. **c** Ni content. **d** Cr content. **e** Si content. **f** O content

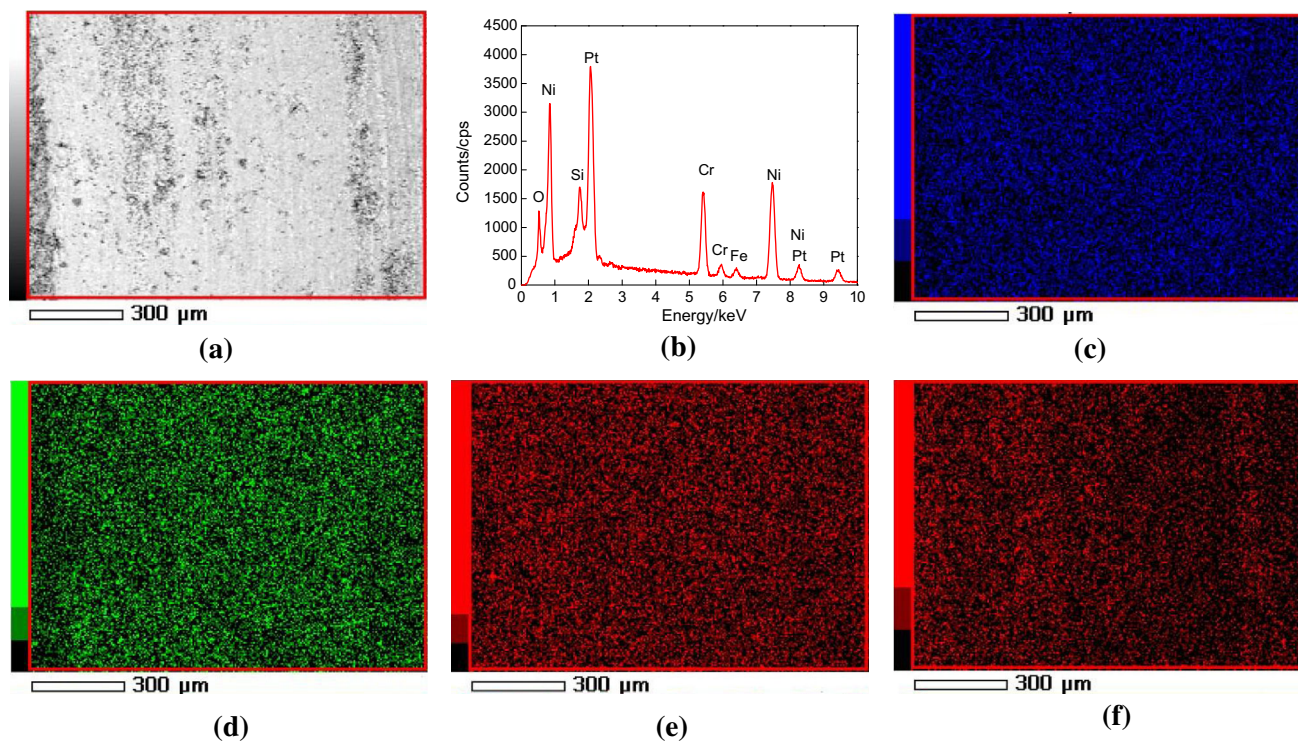


Fig. 11 Plane scan analysis of worn track at 700 °C. **a** Plane scanned position. **b** Result of plane scan analysis. **c** Ni content. **d** Cr content. **e** Si content. **f** O content

content was low. Fe was present on the worn track. This was because a small amount of Fe in the substrate diffused into the NiCrBSi coating. Ni and Si were evenly distributed on the worn track, suggesting that the compounds of Ni and Si were not worn away, as shown in Fig. 10c, e. Cr also formed the atom-rich zone, indicating that the Cr and its compounds had high wear resistance, as shown in Fig. 10d. O content on the worn track increased than that at 500 °C, indicating that the oxidation wear was more severe, as shown in Fig. 10f.

Figure 11a shows the plane scanned position of worn track at 700 °C. The surface of worn track was relatively flat, there were a few furrows along the sliding direction. The result of plane scan analysis is shown in Fig. 11b. The mass fractions of chemical elements (mass%) were: Ni 69.08, Cr 22.04, Si 2.76, O 2.90 and Fe 3.21; and the corresponding atomic fractions were (at%): Ni 60.72, Cr 21.87, Si 5.08, O 9.36 and Fe 2.97. B did not appear in the plane scan result because it is a light element and its content was low. The Fe came from the diffusion of substrate, which could be ignored in the wear test. The distributions of Ni and Si were the same as those at 500 and 600 °C, indicating that the dispersion strengthening effect existed and its high hardness maintained its integrity, as shown in Fig. 10c, e. The Cr distribution was the same as those at 500 and 600 °C, as shown in Fig. 11d. The O content increased than those at 500 and 600 °C and evenly

dispersed on the worn track, as shown in Fig. 11f, indicating that the oxide film was not broken at this time and still played a role in blocking the adhesive wear.

From the above analysis, it could be seen that the Ni, Si and Cr compounds in the NiCrBSi coating was the main factor of wear resistance. Combined with the profiles of worn tracks in Fig. 4b, it was confirmed that the coating could withstand the given test conditions and not be worn out below 700 °C.

4 Conclusions

1. The HVOF sprayed NiCrBSi coating is composed of Ni, NiO, and NiO₂ oxide films after the high temperature wear test, playing a role in reducing COFs.
2. The average COFs of NiCrBSi coating at 500, 600, and 700 °C are 0.4046, 0.4039, and 0.3975, respectively, and the corresponding wear rate increases in multiples with the wear temperatures increasing.
3. The wear mechanism of NiCrBSi coating at 500 and 600 °C is abrasive wear and adhesive wear, accompanied with slight oxidation wear; while that at 700 °C is abrasive wear and oxidation wear.

Acknowledgements Financial support for this research by the Jiangsu Province Science and Technology Support Program (Industry) (BE2014818) is gratefully acknowledged.

References

- Jacobsen S D, Hinrichs R, Aguzzoli C, Figueroa C A, Baumvol I J R, and Vasconcellos M A Z, *Surf Coat Technol* **286** (2016) 129
- Telasang G, Majumdar J D, Padmanabham G, and Manna I, *Surf Coat Technol* **261** (2015) 69
- Wang Y B, Zhao S S, Gao W Y, Zhou C Y, Liu F L, and Lin X C, *J Mater Process Technol* **214** (2014) 899
- Kong D J, and Zhao B G, *J Alloys Compd* **705** (2017) 700
- Sidhu T S, Prakash S, and Agrawal R D, *Mater Sci Eng A* **445–446** (2007) 210
- Sidhu T S, Prakash S, Agrawal R D, Yu H L, Zhang W, Wang H M, Yin Y L, Ji X C, and Zhou K B, *J Alloys Compd* **672** (2016) 137
- Guo C, Chen J, Zhou J, Zhao J, and Wang L, *Surf Coat Technol* **206** (2012) 2064
- Zhu L N, Xu B S, Wang H D, and Wang C B, *Mater Sci Eng A* **528** (2010) 425
- Sidhu T S, Prakash S, and Agrawal R D, *Thin Solid Films* **515** (2006) 95
- Zikin A, Antonov M, Hussainova I, Katona L, and Gavrilović A, *Tribol Int* **68** (2013) 45
- Shabana, Sarcar M M M, Suman K N S, and Kamaluddin S, *Mater Today Proc* **2** (2015) 2654
- Rodriguez J, Martín A, Fernández R, and Fernández JE, *Wear* **255** (2003): 950
- Miguel J M, Guilemany J M, and Vizcaino S, *Tribol Int* **36** (2003) 181
- Karaoglanli A C, Oge M, Doleker K M, and Hotamis M, *Surf Coat Technol* **318** (2017) 299
- Houdková S, Smazalová E, Vostrák M, and Schubert J, *Surf Coat Technol* **253** (2014) 14
- Guo C, Zhou J, Chen J, Zhao J, Yu Y, and Zhou H, *Wear* **270** (2011) 492
- Shabana, Sarcar M M M, Suman K N S, and Kamaluddin S, *Mater Today Proc* **2** (2015) 2654
- Zhu L N, Xu B S, Wang H D, and Wang C B, *Mater Sci Eng A* **536** (2012) 98
- Luo X, Li J, and Li G J, *J Alloys Compd* **626** (2015) 102
- Deschuyteneer D, Petit F, Gonon M, and Cambier F, *Surf Coat Technol* **283** (2015) 162
- Jiang J, Stott FH, and Stack M M, *Wear* **256** (2004) 973
- Pauschitz A, Roy M, and Franek F, *Tribol Int* **41** (2008) 584
- Inman I A, Rose S R, and Datta P K, *Tribol Int* **39** (2006) 1361
- Inman I A, and Datta P S, *Tribol Int* **44** (12) 1902
- Zhou S F, Lei J B, Dai X Q, Guo J B, Gu Z J, and Pan H B, *Int J Refract Met Hard Mater* **60** (2016) 17